International Journal of Mechanical Engineering and Applications
2015; 3(3-1): 40-48
Published online May 12, 2015 (http://www.sciencepublishinggroup.com/j/ijmea)
doi: 10.11648/j.ijmea.s.2015030301.17
ISSN: 2330-023X (Print); ISSN: 2330-0248 (Online)

Geometrical Optimization of Top-Hat Structure Subject to Axial Low Velocity Impact Load Using Numerical Simulation

Hung Anh Ly*, Hiep Hung Nguyen, Thinh Thai-Quang

Department of Aerospace Engineering, Faculty of Transportation Engineering, Ho Chi Minh City University of Technology, Ho Chi Minh City, Vietnam

Email address:
lyhunganh@hcmut.edu.vn (H. A. Ly), nguyenhiephung1992@gmail.com (H. H. Nguyen), quang_thinh1207@yahoo.com (T. Thai-Quang)

To cite this article:
Hung Anh Ly, Hiep Hung Nguyen, Thinh Thai-Quang. Geometrical Optimization of Top-Hat Structure Subject to Axial Low Velocity Impact Load Using Numerical Simulation. *International Journal of Mechanical Engineering and Applications*. Special Issue: Transportation Engineering Technology — part Ⅱ. Vol. 3, No. 3-1, 2015, pp. 40-48. doi: 10.11648/j.ijmea.s.2015030301.17

Abstract: Crashworthiness is one of the most important criteria in vehicle design. A crashworthy design will reduce the injury risk to the occupants and ensure their safety. In structure design, the energy absorption and dispersion capacity are typical characteristics of crashworthy structure. This research continues the previous studies, focuses on analyzing the behavior of top-hat and double-hat thin-walled sections subjected to axial load. Due to limitations on the experimental conditions, this paper focuses on analyzing the behaviors of top-hat and double-hat thin-walled sections by theoretical analysis and finite element method. Two main objectives are setting up finite element models to simulate top-hat and double-hat thin-walled structures in order that the results are consistent with the theoretical predict; and using the results of these models to optimize a top-hat column subject to mean crushing force and sectional bending stiffness constraints by the "Two-step RSM-Enumeration" algorithm. An approximate theoretical solution for a top-hat column with different in thickness of hat-section and closing back plate is also developed and applied to the optimization problem.

Keywords: Crashworthiness, Impact, Optimization, Top-hat

1. Introduction

Crashworthiness is the ability to protect the passengers in case of collision. For example, a helicopter with crashworthy design can guarantee the life of pilots even in cases where the aircraft crashed; or a car impacts at high speed, but the driver's safety is assured thanks to the airbag, seatbelts, and the structures which absorb and disperse impact energy. In structure design, crashworthiness is related to the energy absorption capacity of the structure. Normally, the thin-walled structures made of steel are used for this task. The impact energy is absorbed on the folding wave of the thin-walled structure. To make the design process easier, behaviors of these structures have been studied for many years [1] [2] [3]. This research continues the previous studies, focuses on analyzing the behavior of top-hat and double-hat thin-walled sections subjected to axial load.

In this paper, FE models of top-hat structure is set up and comparing with the theoretical analysis developed by M.D. White *et al.* [4] [5] and Q. Wang *et al.* [6]. Then, the models are used as the data for optimizing a top-hat column subject to mean crushing force and sectional bending stiffness constraints. The "Two-step Response Surface Methodology (RSM) - Enumeration" algorithm introduced by Y. Xiang *et al.* [7] is used in cases of the thickness of hat-section and closing back plate are the same $(\mathbb{SO})_1$ and different $(\mathbb{SO})_2$. The results will be compared and evaluated.

2. Theoretical Review

2.1. Behavior of Top-Hat Section

2.1.1. The Theoretical Analysis of M.D. White et al. and Q. Wang et al.

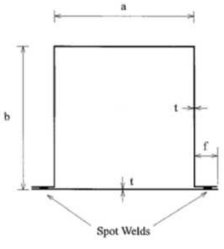

(a)

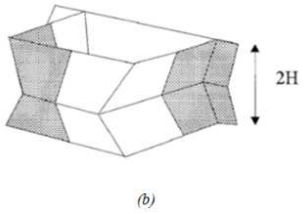

Figure 1. *(a). Cross-section of a top-hat column. (b) Four asymmetric elements forming a collapse profile [2-5].*

Super-folding element model of W. Abramowicz and T. Wierzbicki (as shown in Figure 1) applies to isotropic materials with properties that do not change over time, solid and perfectly plastic; the simple solution is

$$E_{int} = P_m \times \delta_e = \frac{t^2}{4}\left(\sigma_0^{(1)} 8I_1 \frac{r}{t} + \sigma_0^{(2)} \pi \frac{C}{H} + \sigma_0^{(3)} 2I_3 \frac{H}{r}\right) 2H \quad (1)$$

where t is the thickness of section, r is the rolling radius, C is the perimeter of a super-folding element, $2H$ is the length of a folding wave, $\delta_e = 0.73 \times 2H$ is the effective crushing distance, and $\sigma_0^{(i)}$ is the energy equivalent flow stress in the i^{th} region of plastic flow.

By dividing hat-section into four "L" shape super-folding elements, M. D. White *et al.* [4] [5] were able to apply the model of W. Abramowicz and T. Wierzbicki to their analytical solution for a top-hat section with strain hardening materials, which give

$$\frac{\bar{P}_m}{M_u} = 35.55\left(\frac{L}{t}\right)^{0.29} \quad (2)$$

$$\frac{H}{t} = 0.478\left(\frac{L}{t}\right)^{0.64} \quad (3)$$

The general form of the relation between the dynamic crushing force and the mean static crushing force is

$$\frac{(\bar{P}_m)^d}{\bar{P}_m} = 1 + \left(\frac{\dot{\varepsilon}_{av}}{D}\right)^{\frac{1}{p}} \quad (4)$$

The average strain rate during axial crushing of an asymmetric super-folding element which was estimated by W. Abramowicz and T. Wierzbicki [8] is

$$\dot{\varepsilon}_{av} = \frac{tV_m}{4\delta_e r_f} \quad (5)$$

where $V_m = V/2$ is the mean velocity, V is the impact velocity, $r/r_f = 1.36$ and $\delta_e = 0.73H$ ($2\delta_e$ is the final length of a folding wave [9]). The mean dynamic crushing force for a strain hardening, strain rate sensitive top-hat section is

$$\frac{(\bar{P}_m)^d}{\bar{P}_m} = 1 + \left(0.87\frac{V}{L^{0.96}t^{0.04}D}\right)^{\frac{1}{p}} \quad (6)$$

In a different way, Q. Wang *et al.* [6] made the corrections for the theoretical analysis of top-hat section developed by M.D. White *et al*. [4] [5] is

$$(\bar{P}_m)^d = t^2\sigma_0\left(6.08\frac{r}{t} + 1.08\frac{L}{H} + 3.15\frac{H}{r} + \left(\frac{tV}{4.3D}\right)^{\frac{1}{p}}\left(\frac{6.08}{t}H^{-\frac{1}{p}}r^{1-\frac{1}{p}} + 1.08LH^{-1-\frac{1}{p}}r^{-\frac{1}{p}} + 3.15H^{1-\frac{1}{p}}r^{-1-\frac{1}{p}}\right)\right) \quad (7)$$

The same method as the static theoretical prediction was used to obtain the results of parameters H and r by minimizing Eq. (7) respect to H and r, and equaled to zero.

2.1.2. An Approximate Analytical Solution for a Top-Hat Section with Different in Thickness of Hat-Section and Closing Back Plate

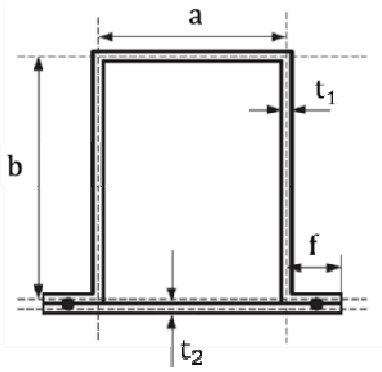

Figure 2. *Cross-section of new top-hat column.*

An approximate analytical solution for a new top-hat section with different in the thickness of hat-section t_1 and the thickness of closing back plate t_2 as shown in Figure 2 can be found by the same Q. Wang's procedure.

The total dissipated energy E_T of top-hat section is the sum of energy dissipated on hat-section E_{hat} and the closing back plate E_{plate}

$$E_T = E_{hat} + E_{plate}$$

The energy absorbed by hat-section is equal to the total dissipated energy on four super-folding elements with the average perimeter $C = L_{hat}/4 = (a + 2b + 2f)/4$. Eq. (1) can be rewritten as

$$(P_m)_{hat} = \frac{\sigma_0 t_1^2}{4}\left(17.76\frac{r}{t_1} + \pi\frac{L_{hat}}{H} + 9.184\frac{H}{r}\right)\frac{2H}{\delta_e} \quad (8)$$

By using Eqs. (4), (5) and (8), the mean dynamic crushing load of hat-section is

$$(P_m)_{hat}^d = \sigma_0 t_1^2\left(6.08\frac{r}{t_1} + 1.08\frac{L_{hat}}{H} + 3.15\frac{H}{r} + \left(\frac{t_1 V}{4.3D}\right)^{\frac{1}{p}}\left(\frac{6.08}{t_1}H^{-\frac{1}{p}}r^{1-\frac{1}{p}} + 1.08L_{hat}H^{-1-\frac{1}{p}}r^{-\frac{1}{p}} + 3.15H^{1-\frac{1}{p}}r^{-1-\frac{1}{p}}\right)\right) \quad (9)$$

Considering the closing back plate, the energy absorbed in crushing process given by M.D. White *et al.* [4] is

$$E_{plate} = \frac{\pi}{2} \times 4 \times M_0 \times (a + 2f) = \frac{t_2^2}{4}\sigma_0 2\pi L_{plate} \quad (10)$$

where $L_{plate} = (a + 2f)$ is the width of the closing back plate. The mean crushing load of the plate for the quasi-static axial crushing force is

$$(P_m)_{plate} = \frac{t_2^2}{4}\sigma_0 \pi L_{plate} \frac{1}{H} \frac{2H}{\delta_e} \quad (11)$$

By using Eqs. (4), (5) and (11), the mean dynamic crushing force of the closing back plate is

$$(P_m)^d_{plate} = \sigma_0 t_2^2 \left(1.08 \frac{L_{plate}}{H} + \left(\frac{t_2 V}{4.3D}\right)^{\frac{1}{p}} 1.08 L_{plate} H^{-1-\frac{1}{p}} r^{-\frac{1}{p}}\right) \quad (12)$$

We assume that the different between H and r in Eqs. (9) and (12) can be neglected. Therefore, the total mean dynamic crushing force of the new top-hat section can be written as

$$(P_m)^d = (P_m)^d_{hat} + (P_m)^d_{plate} \quad (13)$$

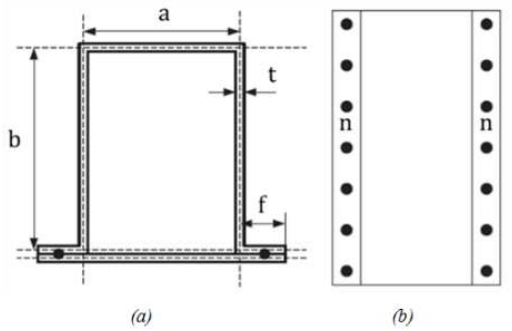

Figure 3. *(a) Cross-section of top-hat column and (b) distribution of spot-weld [7].*

$$(P_m)^d = \sigma_0 \left(\left(6.08 t_1 r + 1.08\, L_{hat} t_1^2 \frac{1}{H} + 3.15 t_1^2 \frac{H}{r}\left(\frac{t_1 V}{4.3D}\right)^{\frac{1}{p}}\left(6.08 t_1 H^{-\frac{1}{p}} r^{1-\frac{1}{p}} + 1.08 L_{hat} t_1^2 H^{-1-\frac{1}{p}} r^{-\frac{1}{p}} + 3.15 t_1^2 H^{1-\frac{1}{p}} r^{-1-\frac{1}{p}}\right)\right)\left(1.08 L_{plate} t_2^2 \frac{1}{H} + \left(\frac{t_2 V}{4.3D}\right)^{\frac{1}{p}} 1.08 L_{plate} t_2^2 H^{-1-\frac{1}{p}} r^{-\frac{1}{p}}\right)\right)$$

with H and r are the root of the set of equations $\partial(P_m)^d / \partial H = 0$ and $\partial(P_m)^d / \partial r = 0$.

2.2. Optimization for Top-Hat Section

Y. Xiang *et al.* [7] introduced the "Two-step RSM-Enumeration" algorithm to optimize the mass of a top-hat column (as shown in Figure 3) subject to mean crushing force P_m and sectional stiffness constraints B. The optimization problem can be written as

$$(\mathbb{SO}) \begin{cases} \min A(x) \\ s.t. \begin{cases} P_m(x, n) \geq \hat{P}_m \\ B(x) \geq \hat{B} \\ x^L \leq x \leq x^U \\ n = 2, 3, \ldots N \end{cases} \end{cases} \quad (14)$$

where A is the cross-sectional area, x is the geometry design variables vector with x^L and x^U are the lower and upper boundary respectively, n is the number of spot-welds on one side, $\hat{P}_m$ and $\hat{B}$ is the smallest allowed values of P_m and B. With the pure finite element approaching, the mean crushing force equation is determined by the RSM method from data of FE models. The "Two-step RSM-Enumeration" optimization method consists of two steps. In the first step, the optimal cross-sectional area with the optimized x^* will be found based on the data of FE top-hat column models with a large number of spot-welds or complete weld. In the second step, the FE top-hat model with the optimal cross-sectional geometry x^* is tested with the increasing number of spot-weld $(n = 2, 3, \ldots N)$ until P_m reaches the desired value.

In this paper, two cases of optimization problem will be carried out and compared. The first optimization problem $(\mathbb{SO})_1$ takes care of the case of normal top-hat section, which is the same with Y. Xiang' case. The second optimization problem $(\mathbb{SO})_2$ takes care of the case of new top-hat section (different in thickness).

The cross-sectional area A and the bending stiffness B given by Y. Xiang *et al.* [7] for the case of normal top-hat section $(\mathbb{SO})_1$ are

$$A = (2a + 2b + 4f)t \quad (15)$$

And

$$B = EI = E\left(\left(f + \frac{h}{6} + \frac{w}{2}\right)h^2 t + \left(\frac{4}{3}f + 2h + \frac{2}{3}w\right)t^3\right) \quad (16)$$

In the case of different in thickness $(\mathbb{SO})_2$, equation of cross-sectional area A and the bending stiffness B are

$$A = (a + 2b + 2f)t_1 + (a + 2f)t_2 \quad (17)$$

$$B = EI = E(\frac{t_1^3(t_1+a)}{12} + \frac{b^3 t_1}{6} + \frac{t_1^3(f-t_1)}{6} + \frac{t_2^3(2f+a)}{12} + 2t_1\left(f-\frac{t_1}{2}\right)\left(\frac{t_1}{2}+t_2-C\right)^2 + t_1(t_1+a)\left(b+\frac{t_1}{2}+t_2-C\right)^2 + t_2(2f+$$
$$at22-C2+2bt1b2+t2-C2 \quad (18)$$

Where

$$C = \left(\frac{t_2^2(2f+a)}{2} + 2t_1\left(f-\frac{t_1}{2}\right)\left(\frac{t_1}{2}+t_2\right) + t_1(t_1+a)\left(b+\frac{t_1}{2}+t_2\right) + 2bt_1\left(\frac{b}{2}+t_2\right)\right)$$
$$/\left(t_1(t_1+a) + 2bt_1 + 2t_1\left(f-\frac{t_1}{2}\right) + t_2(2f+a)\right)$$

3. Finite Element Model

The Belytschko-Tsay 4-node shell elements with 5 integration points is used to simulate column wall with finer mesh size $(2 \times 2\,mm)$. In this study, the wall column material is mild steel RSt37 which was used by S.P. Santosa *et al.* [10] with mechanical properties: Young's modulus $= 200\ GPa$, initial yield stress $\sigma_y = 251\ MPa$, ultimate stress $\sigma_u = 339\ MPa$, Poisson's ratio $\nu = 0.3$, density $\rho = 7830\ kg/m^3$, and the power law exponent $n = 0.12$. The empirical Cowper-Symonds uniaxial constitutive equation constants $D = 6844\ s^{-1}$ and $p = 3.91$. The material model used to simulate mild steel is piecewise linear plasticity. The true stress – effective plastic strain curve of RSt37 steel was calculated from the engineering stress-strain curve of Santosa and was given in Table 1. The nodes in the lowest cross section of the column are clamped.

Table 1. *True stress – Effective plastic strain data of mild steel RSt37.*

Mild steel RSt37	
Effective plastic strain (%)	**True plastic stress (MPa)**
0.0	251
2.0	270
3.9	309
5.8	339
7.7	358
9.6	375
11.4	386
13.2	398

The indenter is modeled solid elements with Young's modulus $E = 200\ GPa$ and Poisson's ratio $\nu = 0.3$. The contact between the indenter and the column is nodes to surface. The contact used for the column wall is single surface to avoid interpenetration of folds generated during axial collapse. The indenter is only permitted to displace in z-axis with the initial velocity V.

Four hexahedron solid elements are used to simulate a spot-weld. Contact spotweld is also used between the surface nodes and the spot-weld elements. The material model used to simulate the spot-weld is spotweld with the same mechanical properties of mild steel RSt37. In fact, after welding, the spot-weld area has different mechanical properties from the original properties of material. However, these differences are ignored in this study due to the limit of experiment.

The boundary conditions are shown in Figure 4.

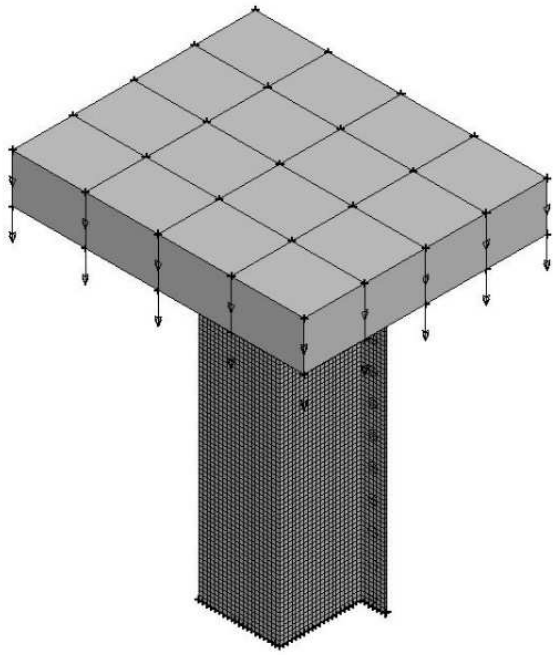

Figure 4. *Boundary conditions.*

4. Results

4.1. The First Optimization Problem

Consider a top-hat column as shown in Figure 3. We want to find the cross-sectional area A such that the weight is minimized subject to mean crushing force P_m and sectional stiffness B constraints with smallest allowed values $\hat{P}_m = 50\ kN$ and $\hat{B} = 4 \times 10^7\ kN\,mm^2$. The column $250\ mm$ in length is under axial crushing by an indenter. Velocity of the indenter is $8\ m/s$. The crushing displacement is $120\ mm$. The column made of mild steel RSt37. The geometry design variables vector $x = (a, b, t, f)^T$ with the limit sizes are $x^L = (40, 40, 0.5, 15)^T$ and $x^U = (80, 80, 0.5, 40)^T$ in mm. The data for optimizing is given in Table 2. The initial values

of a, b, t and f are $60, 60, 2$ and 15 mm, respectively.

Table 2. *Design matrix of* $(\mathbb{SO})_1$.

No.	a (mm)	b (mm)	t (mm)	f (mm)	P_m^{FEM} (kN)	P_m^{Wang} (kN)	Error	P_m^{White} (kN)	Error
1	49.75	40.25	0.77	11.00	11.804	11.442	3.16%	11.725	0.67%
2	58.50	41.25	1.55	14.50	39.277	38.191	2.84%	40.042	1.91%
3	50.00	42.75	2.57	31.25	94.389	93.538	0.91%	99.351	4.99%
4	47.25	43.50	2.76	38.75	107.877	107.783	0.09%	114.432	5.73%
5	77.75	44.50	0.89	28.25	16.774	16.628	0.88%	16.804	0.18%
6	59.00	45.75	1.20	35.00	25.578	27.187	5.92%	27.842	8.13%
7	72.25	46.75	2.07	10.50	64.137	63.335	1.27%	66.965	4.22%
8	60.75	47.75	0.84	15.75	14.250	14.087	1.15%	14.350	0.70%
9	52.75	48.75	0.63	27.00	8.497	8.985	5.43%	9.005	5.64%
10	51.50	50.00	2.33	20.50	79.236	77.529	2.20%	82.312	3.74%
11	74.50	50.50	1.09	37.00	22.690	24.038	5.61%	24.385	6.95%
12	57.00	51.00	2.47	12.50	87.045	83.796	3.88%	89.439	2.68%
13	48.75	52.50	2.98	36.50	124.445	123.709	0.60%	131.563	5.41%
14	42.00	53.25	2.21	14.75	74.415	68.369	8.84%	72.837	2.17%
15	79.75	54.25	2.02	35.50	65.473	67.787	3.41%	70.454	7.07%
16	43.75	56.00	2.55	22.00	92.824	90.333	2.76%	96.228	3.54%
17	65.50	56.00	2.40	24.25	85.985	85.638	0.41%	90.357	4.84%
18	44.75	58.00	2.82	33.25	114.664	111.905	2.47%	118.884	3.55%
19	42.75	58.25	2.30	18.50	76.296	75.186	1.48%	79.890	4.50%
20	70.75	59.50	1.00	34.75	19.716	20.845	5.41%	21.066	6.41%
21	76.00	60.25	1.06	25.25	21.739	22.532	3.52%	22.892	5.04%
22	45.75	61.50	1.82	22.50	53.427	52.337	2.08%	54.848	2.59%
23	75.50	62.00	1.62	26.00	43.767	45.882	4.61%	47.411	7.69%
24	62.50	63.75	1.17	19.25	25.940	25.630	1.21%	26.285	1.31%
25	78.00	64.75	2.17	12.25	76.103	72.066	5.60%	75.773	0.44%
26	63.75	65.25	0.54	29.75	6.813	7.341	7.20%	7.251	6.03%
27	40.25	67.00	2.91	17.25	124.542	112.127	11.07%	120.169	3.64%
28	56.25	67.25	1.43	13.75	35.982	34.933	3.00%	36.259	0.76%
29	55.00	68.75	2.63	27.75	103.062	101.268	1.77%	107.014	3.69%
30	61.50	69.25	1.26	23.50	30.473	29.634	2.83%	30.387	0.28%
31	55.50	70.50	2.73	39.50	111.631	111.986	0.32%	117.855	5.28%
32	73.50	71.50	1.94	32.25	61.310	63.768	3.85%	66.105	7.25%
33	53.75	72.25	1.66	30.50	44.993	47.604	5.49%	49.268	8.68%
34	68.75	73.75	1.70	29.50	48.667	50.601	3.82%	52.256	6.87%
35	64.50	74.25	0.71	24.25	11.650	11.563	0.76%	11.553	0.84%
36	66.50	75.25	1.78	17.50	53.418	52.623	1.51%	54.750	2.43%
37	69.50	76.50	1.49	20.75	39.997	39.790	0.52%	40.992	2.43%
38	46.50	77.50	1.31	16.50	32.350	30.521	5.99%	31.513	2.66%
39	71.50	79.00	1.97	32.75	63.299	65.996	4.09%	68.371	7.42%
40	67.75	79.75	0.59	38.25	9.120	8.941	2.01%	8.797	3.67%

The equation of mean crushing force which formed by RSM algorithm can be written as

$$P_m = 10.9654 - 0.2346a - 0.078b - 0.2868t - 0.0466f - 0.0006ab + 0.018at + 0.0003af + 0.1024bt - 0.0039bf + 0.0228tf + 0.0023a^2 + 0.0014b^2 + 11.8224t^2 + 0.0042f^2 \quad (19)$$

The results in first step of $(\mathbb{SO})_1$ are shown in Table 3. Values of mean crushing force predicted by RSM method and mean crushing force from FE model are approximate.

Table 3. *The optimal cross-sectional dimensions of* $(\mathbb{SO})_1$.

a (mm)	b (mm)	t (mm)	f (mm)	P_m (kN)		B $(10^7\ kN\ mm^2$	A (mm^2)
				RSM	FE		
40	51	1.80	15	50.011	50.298	4.0905	435.6

In the second step of optimization procedure, the FE model with cross-sectional dimensions obtained in the first step is test again with the number of spot-weld $n = 2, 3, ...$ until reaches the expected mean crushing force. As shown in Figure 5, the optimal is top-hat column with 11 spot-welds on each side. Finally, we can conclude that the top-hat column, which has values of cross-sectional dimensions a, b, t and f are $40,\ 51, 1.8$ and 15 mm respectively and 11 spot-welds on each flanges, is the optimum results of $(\mathbb{SO})_1$. Note that in the first step of optimization procedure, if we use the results of mean crushing force from the theoretical solution of Q. Wang *et al.* [6] to find the equation of P_m by RSM method, or use Eqs. (2) and (6) of M.D. White *et al.* [4] [5] directly, we can have results in Table 4. These values are so close. Hence, if the optimization problem does not need high precision, we can use theoretical equations to save the computation time.

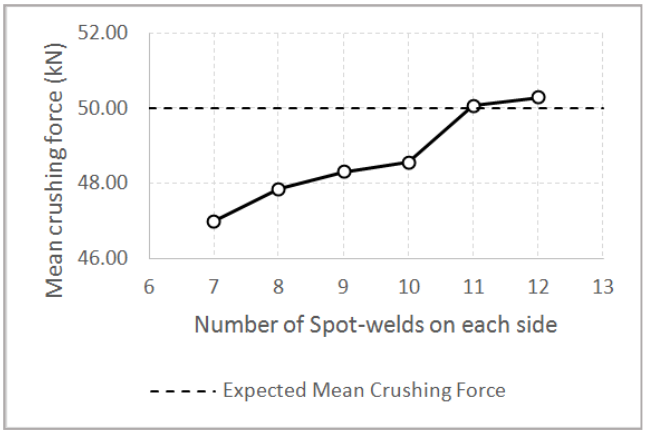

Figure 5. *The second step results of* $(\mathbb{SO})_1$.

Table 4. *Optimization results by three different methods.*

	RSM (from FE results)	RSM (from results of Q. Wang's Eqs.)	Directly from M.D. White's Eqs.
$a\ (mm)$	51	50	51
$b\ (mm)$	40	40	40
$t\ (mm)$	1.80	1.85	1.78
$f\ (mm)$	15	15	15
$A\ (mm^2)$	435.6	444.0	430.8

4.2. The Second Optimization Problem $(\mathbb{SO})_2$

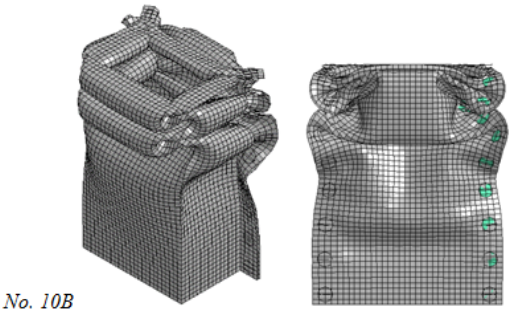

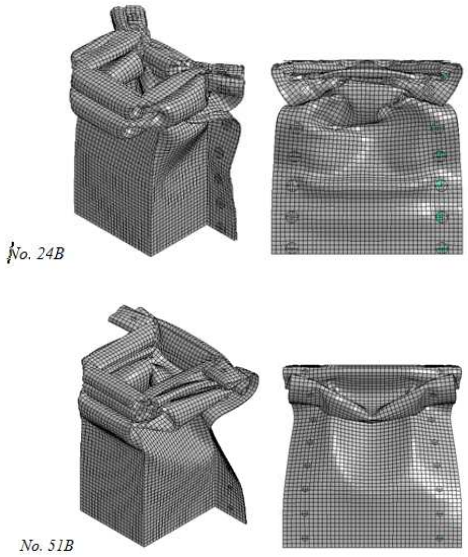

Figure 6. *Deformation of top-hat columns No. 10B, No. 24B, No. 51B.*

In this section, the "Two-step RSM-Enumeration" algorithm is used again to optimize the mass of a new top-hat column subject to $(\mathbb{SO})_1$'s constraints. To reduce the calculation time, Eq. (13) is used to predict the mean crushing force, then correct them to fit with the simulation results. The FE results of 21 top-hat models with different in thickness of hat-section and closing back plate are given in P_m^{FEM} column of Table 5. The models are $250\ mm$ in length, and crushing distance is $120\ mm$. Impact velocity is $8\ m/s$. As shown in Table 5, the difference between result of mean crushing force from approximate theoretical prediction P_m^{ANA} and simulating result P_m^{FEM} is significant when the thickness of hat-section t_1 or the thickness of closing back plate t_2 is much smaller than the perimeter L (in that case, $t < 0.8\ mm$). In addition, when the difference between t_1 and t_2 is significant, the deviation of folding wave of hat-section and the closing back plate becomes more apparent, especially in the case $t_2 < t_1$. Observing the deformation of models No. 10, No. 24 and No. 51 in Figure 6, which have the small t_2/L_{plate} ratio, we can see the buckling phenomenon occurs at the closing back plate. This may be the reason for the decline of P_m in FE models.

Table 5*. Design matrix of* $(\mathbb{SO})_2$.

No.	a (mm)	b (mm)	t_1 (mm)	t_2 (mm)	f (mm)	P_m^{ANA} (kN)	P_m^{FEM} (kN)	P_m^{fixed} (kN)
1	60.50	40.00	1.37	0.89	38.25	31.628	30.004	30.004
2	47.75	41.00	1.59	2.37	21.00	44.344	45.019	45.019
3	44.50	42.00	2.05	1.41	10.00	54.908	58.783	58.783
4	70.50	42.25	0.57	2.42	31.00	14.398		14.416
5	67.00	42.75	2.37	1.28	19.25	74.225	75.816	75.816
6	58.25	43.50	2.67	2.75	37.75	104.205		105.855
7	68.25	44.25	0.94	0.51	13.50	15.689	14.501	14.501
8	58.75	45.00	2.83	1.55	19.75	99.248		97.802
9	41.75	45.75	2.28	1.50	23.75	69.384		68.828
10	77.25	46.25	2.61	1.03	13.75	86.272	83.498	83.498
11	49.00	47.00	2.42	0.94	32.00	77.091		72.316
12	60.00	47.50	0.82	0.81	23.00	13.857		12.939
13	51.75	48.25	1.94	1.85	22.50	56.905		57.285
14	62.25	49.00	1.68	2.48	33.75	53.259		53.613
15	71.25	49.25	2.54	1.30	25.75	86.499	83.495	83.495
16	55.75	50.25	1.11	2.98	27.00	32.718		34.606

No.	a (mm)	b (mm)	t_1 (mm)	t_2 (mm)	f (mm)	P_m^{ANA} (kN)	P_m^{FEM} (kN)	P_m^{fixed} (kN)
17	57.25	51.00	1.00	1.52	13.00	20.573	20.507	20.507
18	40.25	51.75	0.91	2.90	15.25	22.771		26.087
19	65.75	52.50	0.62	2.07	17.00	13.475		13.705
20	64.50	53.00	2.32	1.94	28.75	79.019		77.932
21	53.50	53.75	1.99	2.50	20.75	63.403		66.726
22	72.75	54.50	1.77	2.16	23.25	54.295		54.311
23	46.25	55.25	1.26	1.44	39.75	30.684		29.394
24	75.50	55.50	2.56	0.71	28.00	87.603	82.300	82.300
25	75.25	56.50	2.94	0.86	12.25	106.298		99.918
26	73.50	57.00	1.80	1.76	18.00	52.483		51.818
27	63.25	58.00	1.53	1.83	30.50	42.944		42.033
28	56.50	58.25	1.20	1.36	28.25	27.750		26.687
29	78.50	59.25	2.74	0.99	36.25	101.911	92.038	92.038
30	71.75	59.50	1.87	2.61	15.75	60.290	60.456	60.456
31	47.00	60.75	2.17	1.69	14.75	65.890		67.575
32	73.00	61.00	0.87	2.19	35.50	22.847		22.432
33	43.25	61.50	1.45	2.65	22.00	41.541		44.789
34	63.50	62.50	1.64	1.16	35.75	44.877		42.175
35	50.25	63.25	1.57	2.42	24.25	46.171		48.059
36	64.75	63.50	2.40	1.65	24.75	82.194	82.826	82.826
37	61.75	64.00	1.41	2.72	26.00	43.055		44.653
38	61.00	65.25	2.96	1.99	16.50	113.316	116.791	116.791
39	74.50	65.75	2.22	1.18	25.25	71.934		67.991
40	50.75	66.50	1.03	2.94	34.00	30.624		31.925
41	42.00	67.00	2.49	1.21	29.50	84.205	80.288	80.288
42	52.50	67.50	1.90	2.29	34.50	62.239		62.547
43	69.25	68.50	0.67	2.57	10.50	16.135		17.202
44	54.75	69.00	2.67	0.75	30.50	95.038		88.040
45	41.00	69.50	2.78	0.79	12.00	95.344	91.090	91.090
46	54.25	70.00	2.85	2.23	11.25	106.045		113.448
47	48.25	71.25	2.16	2.12	30.00	72.733		73.433
48	76.50	72.00	1.08	1.88	18.50	26.777	27.805	27.805
49	79.00	72.00	0.51	0.64	32.75	7.314		6.680
50	58.00	72.75	0.79	1.73	36.75	17.980		17.418
51	66.50	73.75	0.72	0.58	32.25	11.727	10.844	10.844
52	77.50	74.50	1.47	2.29	17.25	43.169		43.821
53	53.25	74.75	1.25	2.02	18.00	31.819	33.217	33.217
54	44.00	75.50	2.89	2.67	37.25	119.596		122.987
55	69.25	76.50	1.16	1.04	33.50	26.670		24.902
56	45.00	77.25	1.75	2.85	26.75	57.156	59.366	59.366
57	50.00	77.50	1.32	1.09	39.00	32.378		30.413
58	46.00	78.25	2.12	2.80	14.25	70.941		79.738
59	79.50	78.75	0.64	1.61	39.50	14.156		13.445
60	67.50	80.00	2.04	0.58	20.25	61.578	50.201	50.201
61	40.00	57.25	1.91	0.50	15.00	49.593	44.057	44.057

In this study, for simplicity, we assume that the decrease of the mean crushing force is just affected by the t_2/L_{plate} ratio. The linear relationship between mean force error ε and the t_2/L_{plate} shown in Figure 7 can be written as

$$\varepsilon = 6.3537\left(\frac{t_2}{L_{plate}}\right) - 0.1148 \qquad (20)$$

by linear least squares algorithm from the results of FE models.

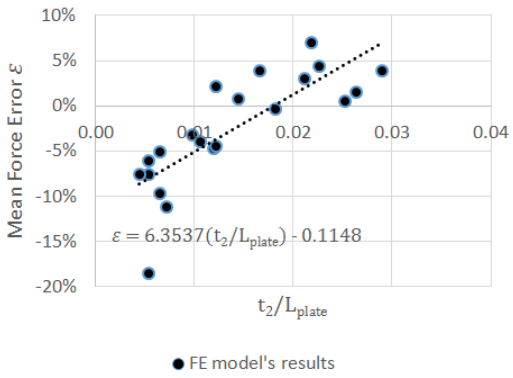

Figure 7. *Mean force error vs.* t_2/L_{plate} *ratio.*

Since then, we have the P_m^{fixed} column in Table 5. P_m^{fixed}

is equaled to P_m^{FEM} if P_m^{FEM} exist, or is calculated by the relationship shown in Eq. (20). The equation of mean crushing force which formed by RSM algorithm from values of P_m^{fixed} can be written as

$$P_m = -22.2942 + 0.3846a + 0.2195b + 7.4044t_1 + 2.0747t_2 - 0.1477f - 0.0019ab - 0.0233at_1 - 0.0321at_2 + 0.002af + 0.055bt_1 + 0.0395bt_2 + 0.0007bf + 3.0142t_1t_2 + 0.0099t_1f - 0.0324t_2f - 0.0015a^2 - 0.0019b^2 + 7.8856t_1^2 + 0.3245t_2^2 + 0.0019f^2 \quad (21)$$

Table 6. *Optimal cross-sectional dimensions of* $(\mathbb{SO})_2$.

a (mm)	b (mm)	t_1 (mm)	t_2 (mm)	f (mm)	P_m (kN)		B $(10^7\ kN\ mm$	A (mm^2)
					RSM	FE		
40	55.75	2.05	0.5	15	50.016	50.211	4.0048	407.075

The results in first step of $(\mathbb{SO})_2$ are given in Table 6. The new cross-sectional area $(407.075\ mm^2)$ is smaller than the older $(435.6\ mm^2)$ about 6.55%.

In second step of $(\mathbb{SO})_2$, as shown in Figure 8, the top-hat column with 12 spot-welds or more on each flange will satisfy the requirement about mean crushing force.

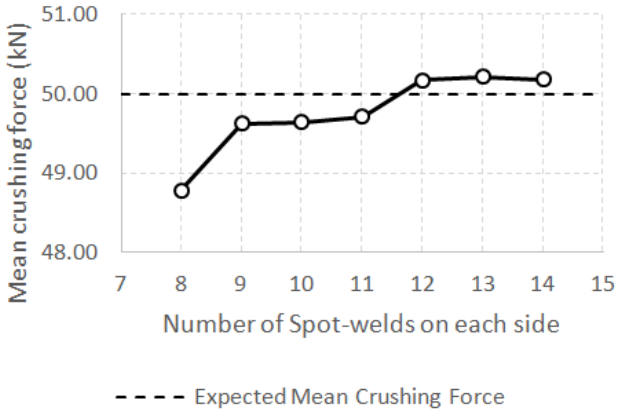

Figure 8. *The second step results of* $(\mathbb{SO})_2$.

Therefore, the top-hat column, which has values of cross-sectional dimensions a, b, t_1, t_2 and f are 40, 55.75, 2.05, 0.5 and 15 mm respectively and 12 spot-welds on each flanges, is the optimum results of $(\mathbb{SO})_2$. 6.55% mass of the optimal top-hat column of $(\mathbb{SO})_1$ has been reduced. Note that the equation of mean crushing force Eq. (23) used in the first step of $(\mathbb{SO})_2$ is based on data from the approximate theoretical solution corrected by FE models. Therefore, this optimal result of $(\mathbb{SO})_2$ may not be the most optimal result. That mean the most optimal result can coincide with this result or can give the smaller cross-sectional area (a little more better).

5. Conclusions

In this paper, the theoretical predictions for behavior of top-hat thin-walled structure are used as a basis for checking the correctness of the model. Results of the investigation of spot-weld pitch show that when the spot-weld pitch decreases, the mean crushing force will be increased to the saturation value which approximates to the analytical result. The value of spot-weld pitch that mark the start of the saturation region is equaled to $1.0H$. In optimization problem for a top-hat column, using the results of mean crushing force from the theoretical solution of Q. Wang et al. to find the equation of P_m by RSM method, or use Eqs. (2) and (6) of M.D. White et al. directly in the first step of "Two-step RSM-Enumeration" algorithm can help to save significant computation time if the optimization problem does not require high accuracy. Allowing the different in thickness of hat-section and closing back plate in optimization problem can help improve the energy absorption capacity of top-hat structures in case the weight is no change, mean that the weight can be reduce (about 6.55% for the problem in this paper). The theoretical analysis for top-hat thin-walled section with different in thickness of hat-section and closing back plate is quite suitable in the case of deformation of the flanges and the closing back plate is similar. Results of this theory should be calibrated with experimental results.

Acknowledgements

The research for this paper was financially supported by AUN/SEED-Net, JICA for CRA Program.

Nomenclature

$2H$	length of a folding wave
a	width of a top-hat section
b	depth of a top-hat section
B	sectional bending stiffness
D, p	Cowper-Symonds coefficients
E	Young's modulus
E_{int}	internal energy absorbed by a super-folding element in asymmetric folding mode
E_{plate}	energy absorbed by the closing back plate
E_{hat}	energy absorbed by the hat-section
E_T	total energy absorbed
f	width of flange
I	second moment of area
L	perimeter of a top-hat section
P_m	mean crushing force
r	rolling radius of toroidal surface
t	thickness of section
δ_e	effective crushing distance
σ_0	flow stress of material

Reference

[1] W. Abramowicz and N. Jones, "Dynamic axial crushing of circular tubes," *International Journal of Impact Engineering*, vol. 2, no. 3, pp. 263-281, 1984.

[2] W. Abramowicz and N. Jones, "Dynamic axial crushing of square tubes," *International Journal of Impact Engineering*, vol. 2, no. 2, pp. 179-208, 1984.

[3] W. Abramowicz and N. Jones, "Dynamic progressive buckling of circular and square tubes," *International Journal of Impact Engineering*, vol. 4, no. 4, pp. 243-270, 1986.

[4] M. White, N. Jones and W. Abramowicz, "A theoretical analysis for the quasi-static axial crushing of top-hat and double-hat thin-walled section," *International Journal of Mechanical Sciences,* vol. 41, pp. 209-233, 1999.

[5] M. White, N. Jones, "A theoretical analysis for the dynamic axial crushing of top-hat and double-hat thin-walled sections," *Proceedings of the Institution of Mechanical Engineers,* vol. 213, pp. 307-325, 1999.

[6] Q. Wang, Z. Fan and L. Gui, "A theoretical analysis for the dynamic axial crushing behavior of aluminium foam-filled hat sections," *International Journal of Solids and Structures,* vol. 43, pp. 2064-2075, 1999.

[7] Y. Xiang, Q. Wang, Z. Fan and H. Fang, "Optimal crashworthiness design of a spot-weld thin-walled hat section," *Finite Elements in Analysis and Design,* vol. 42, pp. 846-855, 2006.

[8] W. Abramowicz and T. Wierzbicki, "Axial crushing of multicorner sheet metal columns," *Journal of Applied Mechanics,* vol. 56, no. 1, pp. 113-120, Mar. 1989.

[9] W. Abramowicz, "The effective crushing distance in axially compressed thin-walled metal columns," *International Journal of Impact Engineering,* vol. 1, no. 3, pp. 309-317, 1983.

[10] S. P. Santosa, T. Wierzbicki, A. G. Hanssen and M. Langseth, "Experimental and numerical studies of foam-filled sections," *International Journal of Impact Engineering,* vol. 24, pp. 509-534, 1999.

Biography

Hung Anh Ly is a lecturer in the Department of Aerospace Engineering – Faculty of Transport Engineering at Ho Chi Minh City University of Technology (HCMUT). He received his BEng in Aerospace Engineering from HCMUT in 2005, his MEng in Aeronautics and Astronautics Engineering from Bandung Institute of Technology - Indonesia (ITB) in 2007 and his DEng in Mechanical and Control Engineering from Tokyo Institute of Technology - Japan (Tokyo Tech) in 2012. He is a member of the New Car Assessment Program for Southeast Asia (ASEAN NCAP). His main research interests include strength of structure analysis, impact energy absorbing structures and materials.

Hiep Hung Nguyen received the Bachelor of Engineering in Aerospace of Engineering with Second Class Honours from Ho Chi Minh City University of Technology (HCMUT), Vietnam in April, 2015. He spent two years studying in the field of impact of thin-walled structures. His expertise is structural analysis using finite element method.

Thinh Thai-Quang received the Bachelor of Engineering in Aerospace of Engineering with First Class Honours from Ho Chi Minh City University of Technology (HCMUT), Vietnam in April, 2015. His research interests include the areas of structural impact, finite element methods, and structural mechanics.